Heliyon 9 (2023) e21006

Contents lists available at ScienceDirect

Heliyon

journal homepage: www.cell.com/heliyon

Cloning, expression, and biochemical characterization of β-etherase LigF from *Altererythrobacter* sp. B11

Marcela Robles-Machuca [a,1], Lucero Aviles-Mejía [b,1], Itzel Celeste Romero-Soto [b], Jorge A. Rodríguez [c], Vicente Paúl Armenta-Pérez [c], María Angeles Camacho-Ruiz [b,*]

[a] *Tecnología de Alimentos, Secretaría de Investigación y Posgrado, Universidad Autónoma de Nayarit, Tepic, 63000, Nayarit, Mexico*
[b] *Laboratorio de Investigación en Biotecnología, Centro Universitario del Norte, Universidad de Guadalajara, Colotlán, 46200, Jalisco, Mexico*
[c] *Biotecnología Industrial, Centro de Investigación y Asistencia en Tecnología y Diseño del Estado de Jalisco (CIATEJ), Zapopan, 45019, Jalisco, Mexico*

ARTICLE INFO

Keywords:
Lignin
Lignin depolymerization
Biorefinery
Biochemical characterization
β-etherases

ABSTRACT

Lignin, a complex heteropolymer present in plant cell walls, is now recognized as a valuable renewable resource with potential applications in various industries. The lignin biorefinery concept, which aims to convert lignin into value-added products, has gained significant attention in recent years. β-etherases, enzymes that selectively cleave β-*O*-4 aryl ether bonds in lignin, have shown promise in lignin depolymerization. In this study, the β-etherase LigF from *Altererythrobacter* sp. B11 was cloned, expressed, purified, and biochemically characterized. The LigF-AB11 enzyme exhibited optimal activity at 32 °C and pH 8.5 when catalyzing the substrate PNP-AV. The enzyme displayed mesophilic behavior and demonstrated higher activity at moderate temperatures. Stability analysis revealed that LigF-AB11 was not thermostable, with a complete loss of activity at 60 °C within an hour. Moreover, LigF-AB11 exhibited excellent pH stability, retaining over 50 % of its activity after 1 h under pH conditions ranging from 3.0 to 11.0. Metal ions and surface impregnation agents were found to affect the enzyme's activity, highlighting the importance of considering these factors in enzymatic processes for lignin depolymerization. This study provides valuable insights into the biochemical properties of LigF-AB11 and contributes to the development of efficient enzymatic processes for lignin biorefineries. Further optimization and understanding of β-etherases will facilitate their practical application in the valorization of lignin.

1. Introduction

Lignin, a complex heteropolymer abundant in plant cell walls, has traditionally been considered an undesirable byproduct in industries such as pulp and paper. However, in recent years, there has been a significant shift in perspective, with lignin being recognized as a valuable renewable resource with immense potential. The concept of lignin biorefinery has emerged, aiming to harness the unique chemical structure of lignin and convert it into value-added products [1,2]. Lignin is primarily composed of phenylpropanoid units, such as coniferyl alcohol, sinapyl alcohol, and *p*-coumaryl alcohol [3]. These units are linked by chemical bonds, predominantly aryl

* Corresponding author.
E-mail addresses: marcela.robles@uan.edu.mx (M. Robles-Machuca), angeles_camacho@cunorte.udg.mx (M.A. Camacho-Ruiz).
[1] These authors contributed equally to the development of the work.

https://doi.org/10.1016/j.heliyon.2023.e21006
Received 11 July 2023; Received in revised form 25 September 2023; Accepted 12 October 2023
Available online 14 October 2023

ether, and carbon-carbon bonds, forming a three-dimensional network that provides rigidity and strength to plants [4].

Efficient depolymerization of lignin involves breaking the chemical bonds within its structure to obtain lower molecular weight and simpler compounds. Among the products obtained are aromatic monomers, such as vanillic acid, syringic acid, ferulic acid, and ρ-coumaric acid, which can serve as precursors for the production of a wide range of chemicals, including resins, adhesives, polymers, and fragrances [2].

One such class of enzymes that has shown promise in lignin depolymerization is β-etherases, which belong to the glutathione S-transferase family and rely on glutathione as a co-substrate [5]. Unlike oxidoreductase enzymes such as laccases and peroxidases, which generate phenoxy radicals prone to polymerization, β-etherases possess the unique ability to selectively cleave β-*O*-4 aryl ether bonds [6,7], which represent approximately 45–60 % of the total bonds present in lignin [8]. The Sphingomonad pathway for β-aryl ether bond cleavage in model lignin substrates consists of three steps. It begins with the selective oxidation of a hydroxyl group at the α position of the β-*O*-4 aryl ether bond, catalyzed by alcohol dehydrogenases [5,9]. Once the ketobenzylic group is formed, β-etherases can act with high stereoselectivity on the adjacent β-*O*-4 aryl ether bond. Subsequently, glutathione lyases act on chiral glutathione adducts, resulting in the cleavage of the thioether bond and the release of oxidized glutathione [9–13].

The β-etherase activity has been described in bacterial systems since the 1970s [14,15]; however, it was not until 1989 that Masai et al. [16] first detected and localized the β-etherase enzyme in the SYK-6 strain of *Pseudomonas paucimobilis*, which was later renamed as *Sphingobium* sp. SYK-6 [9,10,16]. Since then, numerous studies have been conducted to characterize different types of β-etherases based on their sequence homology, including types LigE, LigF, LigP, and BaeAB each exhibiting distinct enantiomeric selectivity [10–12,17].

Biochemical characterization of β-etherases is essential for their practical application. Previous studies have explored the pH and temperature optima for various recombinant β-etherases expressed in *Escherichia coli*. Reiter et al. [18] reported that the β-etherase LigF from *Sphingobium* sp. SYK-6 exhibited higher activity at pH 10.0 and a temperature of 60 °C in the transformation of the model lignin substrate 1-(4-hydroxy-3-methoxyphenyl)-2-(2-methoxyphenoxy)-1,3-propanediol (guaiacylglycerol- β-guaiacyl ether). Picart et al. [12] cloned and characterized the β-etherases LigE, LigF, and LigP from *Sphingobium* sp. SYK6, as well as LigF-NS and LigE-NS from *Novosphingobium* sp. PP1Y, LigF-NA and LigE-NA from *N. aromaticovorans* DSM 12444, and LigP-SC from *Sorangium cellulosum* So Ce56. They found that all these enzymes exhibited maxima activity at temperatures between 20 and 30 °C and pH value between 9.0 and 9.5 in the transformation of the substrate guaiacyl-α-veratrylglycerone. Recently, Voβ et al. [19] cloned and characterized several β-etherases, including LigE and LigF from strains of the genera *Altererythrobacter*, *Sphingomonas*, *Novosphingobium*, *Sphingobium*, and *Erythrobacter*, as well as a Gammaproteobacteria. They observed that all these enzymes exhibited an optimal pH of 9, while the optimal temperature varied between 20 and 40 °C in the catalysis of the substrate β-(2,6-dimethoxyphenoxy)-α-veratrylglycerone.

Researchers have made efforts to design biocatalytic processes for lignin depolymerization based on the biochemical properties of β-etherases. Reiter et al. [18] investigated the enzymatic system of *Sphingobium* sp. SYK-6, which included LigD, LigF, and LigG enzymes involved in releasing lignin monomers from complex natural lignin structures. In their study, the researchers used softwood/hardwood alkali-lignins and bagasse organosolv-lignin as substrates and observed minimal release of monolignins after a 50-h reaction period. In a separate study, Picart et al. [20] demonstrated the potential of laccase and β-etherases for lignin depolymerization. They utilized β-etherases LigE from *Spingobium* sp. SYK6, LigF-NA from *Novosphingobium aromaticivorans*, and the glutathione lyase LigG-TD from *Thiobacillus denitrificans* to achieve a significant yield in the depolymerization of OrganoCat beech wood lignin. The researchers emphasized the importance of optimizing the process to increase yields.

Developing efficient enzymatic processes for lignin depolymerization requires determining and utilizing the optimal conditions for each specific enzyme, as well as investigating their stability under different temperature and pH conditions. Additionally, the influence of various effectors that can inhibit or activate their catalytic function needs to be analyzed [21]. It has been observed that certain ions, such as Cd^{+2}, Cu^{+2}, Zn^{+2}, and Ag^{+} [22], as well as specific chelating agents like EDTA [23], can interact with the amino acids of the enzyme, resulting in alterations in the active site and subsequent activation or inactivation [24].

In this context, our study centers on the comprehensive exploration of β-etherase LigF from *Altererythrobacter* sp. B11. This particular microorganism holds a distinct position of interest, belonging to the alphaproteobacterium classification within the family Sphingomonadaceae. *Altererythrobacter* has earned recognition as a proficient lignin degrader, playing a crucial role in the breakdown of phenolic compounds derived from lignin [25,26]. Notably, Voβ et al. [19] reported that β-etherases LigE and LigF from *Altererythrobacter* exhibited two to three times higher activity levels compared to those from *Sphingobium* sp SYK-6, thus accentuating the significance of their in-depth characterization.

Furthermore, LigF, in conjunction with LigE, constitutes a distinct subclass of β-etherases that has garnered considerable attention. This heightened interest is attributed to their remarkable enantiomeric selectivity. While this selectivity offers advantages for targeted lignin degradation, it also presents intricate challenges that demand a meticulous investigation into their properties. Consequently, our investigation into LigF from *Altererythrobacter* sp. B11 promises to contribute significantly to our understanding of lignin-degrading enzymes and their prospective applications.

2. Materials and methods

2.1. Identification of novel β-etherase

The sequence encoding for β-etherase was discovered through an extensive search of the publicly accessible GenBank nr database from NCBI, utilizing the basic local alignment search tool (BLAST) algorithm. The database was examined using the amino acid sequences of β-etherase LigF (GenBank: BAA02031.1) derived from *Sphingobium* sp. SYK6. A closely related protein (66.26 % identity),

LigF-AB11 (GenBank: BBC73091.1), was chosen for further analysis (Fig. 1).

A phylogenetic tree was constructed to position LigF-AB11 within the context of its evolutionary relationship with other known or predicted glutathione S-transferases (GSTs) involved in catalyzing reactions associated with the sphingomonad pathway for breaking the β-aryl ether bond, as reported by Kontur et al. [17]. The nucleotide sequences of these enzymes were aligned using the MUSCLE (Multiple Sequence Comparison by Log-Expectation) algorithm, and the phylogenetic tree was generated using the Neighbor-Joining method. To assess the robustness of the phylogenetic groupings, 1000 bootstrap replicates were performed. Both analyses were conducted using MEGA version 11.0.13 (Fig. 2).

2.2. Gene cloning

The LigF-AB11 gene was synthesized by GenScript® (USA) with codon optimization specifically for *E. coli* and subsequently cloned into a pET28a(+) vector using *Nde*I (5′) and *Bam*HI (3′) restriction sites. This cloning strategy enabled the addition of a 6X N-terminal His tag. Expression of the enzyme was performed in the *E. coli* BL21(DE3) strain. The bacterial culture was cultivated in Luria-Bertani broth medium (LB) supplemented with kanamycin (30 mg/L) at 37 °C and 250 rpm until it reached an optical density at $\lambda = 600$ nm of approximately 0.9. Subsequently, the culture was induced with 0.5 mM isopropyl-β-D-thiogalactopyranoside (IPTG) and the expression was carried out overnight at 16 °C and 250 rpm.

A cell pellet was obtained via centrifugation and subjected to cell lysis using 425–600 μm glass beads (30–40 U S. sieve). The active enzyme was extracted from the lysed cells using 25 mM Tris buffer at pH 8.0 and recovered in the supernatant (cell-free culture).

2.3. Enzyme purification

For enzyme purification, the overexpressed cells were resuspended in a binding buffer (50 mM sodium phosphate buffer, pH 8.0, 300 mM NaCl, 10 mM imidazole) and sonicated to lyse them. After centrifugation to remove cell debris, the resulting cell lysate was applied to a HIS-Select HF nickel-sepharose affinity column to purify the His-tagged enzymes using a peristaltic pump at a flow rate of 1 mL/min. The His-tagged enzymes were eluted from the column using an elution buffer (50 mM sodium phosphate buffer, 300 mM NaCl, 250 mM imidazole; pH 8.0). The protein fractions obtained underwent analysis using sodium dodecyl sulfate polyacrylamide gel electrophoresis (SDS-PAGE) and Coomassie staining to confirm the presence and purity of the recombinant enzymes. Fractions containing the purified enzyme were combined and subjected to washing through ultrafiltration using a 10 kDa membrane and a 10 mM phosphate buffer at pH 8.0. Finally, quantification of the purified enzyme was performed using the Bradford assay.

2.4. Enzyme-substrate docking

Protein modeling of LigF-AB11 was conducted using the SWISS-MODEL online server (https://swissmodel.expasy.org), with the LigF structure from *Sphingobium* sp. SYK-6 (PDBID: 4xt0.1.A) serving as the template. The structures of the substrates, 1-(4-hydroxy-3-methoxyphenyl)-2-(4-nitrophenoxy)-etan-1-one (PNP-AV) and (S)-3-hydroxy-1-(4-hydroxy-3-methoxyphenyl)-2-(methoxyphenoxy)-propan-1-one ((S)-GVG), were generated using MarvinSketch software v. 18.5 and optimized with Avogadro software [27]. Molecular docking was performed utilizing AutoDockVina software [28] in conjunction with AutoDockTools [29]. The protein was treated as rigid, while the ligands and the nucleophile Ser110 were considered flexible. The grid center was positioned within a confined 20 × 20

```
    LigF  LKLYSFGPGANSLKPLATLYEKGLEFEQVFVDPSKFEQHSDWFKKINPRGQVPALWHDGK  62
LigF-AB11 ............M..ML..F.....Y..HLL......H.......V.........VDGD.  61

    LigF  VVTESTVICEYLEDVFPESGNSLRPADPFKRAEMRVWTKWVDEYFCWCVSTIGWAFGIKA  122
LigF-AB11 ..............AH.-TEVK...D..YD..Q.....................HR.VRH  120

    LigF  IAQKMSDEEFEEHINKNVPIPEQQLKWRRARNGFPQEMLDEEFRKVGVSVARLEETLSKQ  182
LigF-AB11 M...LT.A.....L-..I.............E....DL....M..I....RK.DDH.ADH  179

    LigF  DYLVDTGYSLADICNFAIANGLQRPGGFFGDYVNQEKTPGLCAWLDRINARPAIKEMFEK  242
LigF-AB11 EW.AGEMFT.......S....M.---NG.AEL..TSD..H.VR.IEQ.....KVR.....  236

    LigF  SKREDL  248
LigF-AB11 VP..R.  242
```

Fig. 1. Alignment of the LigF amino acid sequence from *Altererythrobacter* sp. B11 (ID: BBC73031.1) with the known LigF sequence from Sphingobium sp. SYK-6 (ID: BAA02031.1). Identities are represented by dots: 163/246 (66 %). Gaps are represented by hyphen: 5/246(2 %).

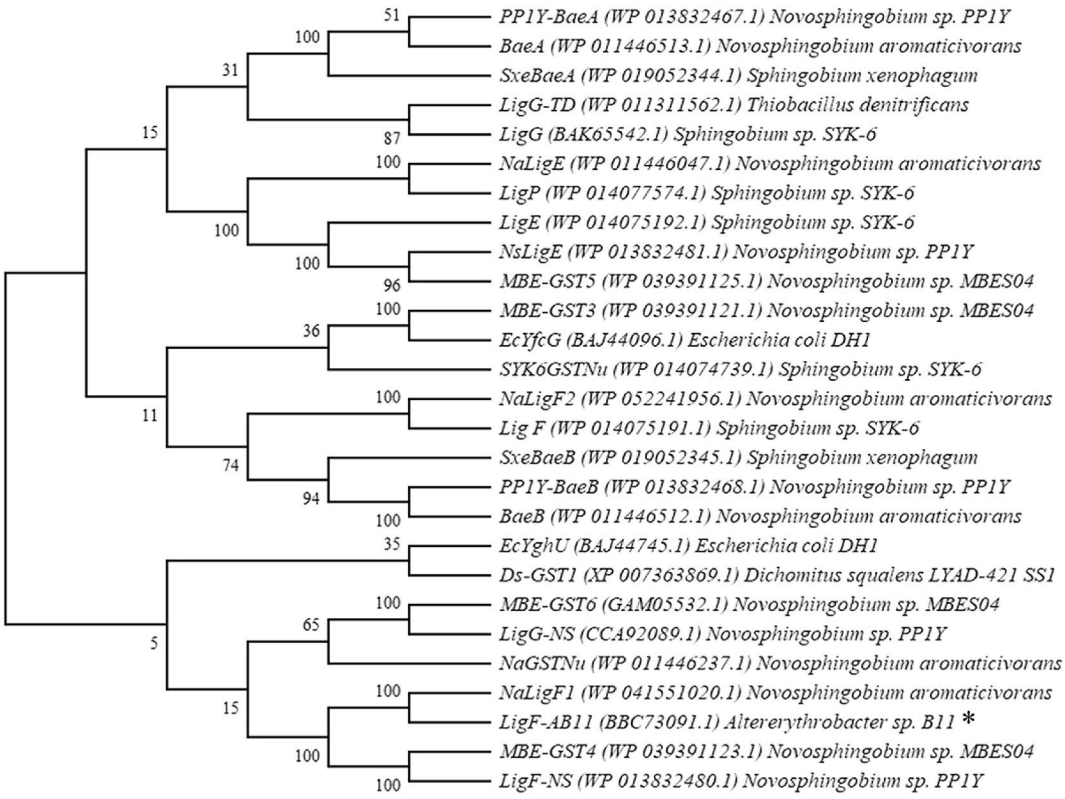

Fig. 2. Phylogenetic tree of known or predicted glutathione S-transferases involved in the sphingomonad pathway for β-aryl ether bond cleavage. LigF-AB11 is denoted by an asterisk (*). The phylogenetic tree was constructed using the neighbor-joining method, utilizing their nucleotide sequences. Bootstrap values (from 1000 replicates) are displayed at the nodes.

× 20 Å region surrounding the GSH binding site. The most energetically favorable pose (kcal/mol) of the substrates, corresponding to the reported orientation by Ref. [13], was compared.

2.5. Chemical synthesis of the PNP-AV

In a 250 mL round-bottom flask, 1.157 g (8.31 mmol) of 4-nitrophenol and 2.25 g (16.28 mmol) of K_2CO_3 were combined with 60 mL of acetone. The mixture was refluxed with constant stirring for 10 min. Then, 2 g (7.96 mmol) of 2-Br-1-(4-hydroxy-3-methoxyphenyl)-etanone dissolved in 20 mL of acetone was added. The reaction proceeded for 2 h. Subsequently, the mixture was filtered using a 0.22 μM PVDF membrane to remove carbonates and evaporated under reduced pressure. The compounds were suspended in ethyl acetate and washed twice with 1 M NaOH, twice with water, and once with brine. The sample was then dried using molecular sieves, filtered, and evaporated under reduced pressure. Finally, the compound was dissolved in 100 mL of hot ethanol and left in a crystallizer to obtain crystals of β-(*p*-nitrophenoxy)-α-acetovanillone (PNP-AV).

To determine the purity of the substance and isolate PNP-AV, an analytical and preparative High-Performance Thin-Layer Chromatography (HPTLC) was utilized. This method utilized chromatoplates measuring 20 × 20 cm, coated with silica 60 (F254), and a mobile phase consisting of ethyl acetate/hexane (70:30, v/v). Following separation, the chromatographic plate was examined under UV light to assess the purity of PNP-AV, with assistance from GelAnalyzer 19.1 software. Subsequently, the pure fraction of PNP-AV was subjected to further analysis. For in-depth structural elucidation, comprehensive 1D and 2D NMR experiments were conducted using a Bruker Avance III 600 NMR spectrometer operating at 14.1 T.

2.6. Activity assay

The β-etherase activity of LigF-AB11 towards PNP-AV was determined by indirectly quantifying the amount of released ρ-nitrophenol through spectrophotometry in a 96-well microplate. The assay mixture comprised 20 μL of enzyme solution, 50 μL of glutathione (12 mM in 25 mM Tris-HCl, pH 8.5), and 50 μL of PNP-AV suspension (2 mM in 25 mM Tris-HCl, 4 % v/v DMSO; pH 8.5). The kinetic assay was conducted at 37 °C for 15 min, with data collected every 30 s at $\lambda = 410$ nm after 5 s of prior agitation. One enzyme unit (U) corresponds to the amount of LigF-AB11 that catalyzes the release of 1 μmol of ρ-nitrophenolate per minute.

2.7. Effect of temperature and pH on the LigF-AB11 activity

The enzymatic activity of the purified enzyme was assessed over a temperature range of 20–80 °C using the spectrophotometric method. To explore the pH effect, a 40 mM Britton-Robinson buffer was substituted for Tris-HCl buffer, with pH values ranging from 5.0 to 10.0. Endpoint assays were carried out, and the reaction was terminated after 10 min of incubation using 200 mM NaOH. Three replicates were conducted for all measurements, and the relative activity was calculated considering the highest measurement considered as 100 %.

2.8. Effect of temperature and pH on enzyme stability

The thermal stability of β-etherase LigF-AB11 was assessed over a temperature range of 30 to 60 °C. For this regard, 16 μg of purified enzyme suspended in 20 μL of Tris-HCl buffer (50 mM, pH 8.5) were incubated at the designated temperature. For the pH stability assays, 16 μg of purified enzyme were incubated in 20 μL of Britton-Robinson buffer (40 mM) at various pH levels, spanning from pH 3.0 to pH 11.0, at 25 °C.

In all instances, the residual activity was measured at pH 8.5 following time intervals of 0, 30, 60, 120, 180, and 240 min. The enzymatic activity measured at the start of the each incubation period for each condition was considered as 100 %. Three independent assays were conducted for each case.

2.9. Activators and inhibitors assays

An enzymatic inhibition analysis was performed by measuring the catalytic activity of LigF-AB11 in the presence of different metallic ions, as well as oxidizing, reducing, and surface impregnating agents. The metallic ions used were $MnSO_4$, $CaCl_2$, $MgCl_2$, NaCl, KCl, $FeCl_2$, $ZnSO_4$, $Pb(NO_3)_2$, and $CuSO_4$. In a 96-well microplate, triplicates of 20 μL of LigF-AB11 enzyme at a concentration of 0.8 mg/L were dispensed. 50 μL of 12 mM glutathione in 25 mM Tris-HCl buffer, pH 8.0, was added. Subsequently, 10 μL of each metallic ion at a final concentration of 1 mM was added, and the mixture was incubated with constant agitation for 5 min to allow the interaction of the ions with the enzyme. Additionally, the effect of oxidizing, reducing, and surface impregnating agents were evaluated at a final concentration of 0.1 mM, including N,N,N′,N′-Tetramethylethylenediamine (TEMED), urea, ethylenediaminetetraacetic acid (EDTA), DL-dithiothreitol (DTT), sodium dodecyl sulfate (SDS), and sodium persulfate.

The residual activity was spectrophotometrically evaluated by adding 50 μL of PNP-AV suspension (2 mM in 25 mM Tris-HCl buffer, 4 % v/v DMSO, pH 8.0).

3. Results and discussion

3.1. Gene identification and phylogenetic analysis of LigF-AB11

The gene used in this investigation was systematically identified through a thorough search within the publicly accessible GenBank nr database hosted by NCBI. This quest relied upon the utilization of the Basic Local Alignment Search Tool (BLAST) algorithm to align the amino acid sequences with that of the extensively studied β-etherase LigF (GenBank: BAA02031.1), originally derived from *Sphingobium* sp. SYK6. The outcome of this alignment unveiled a similarity of approximately 66.26 % between the LigF-AB11 gene

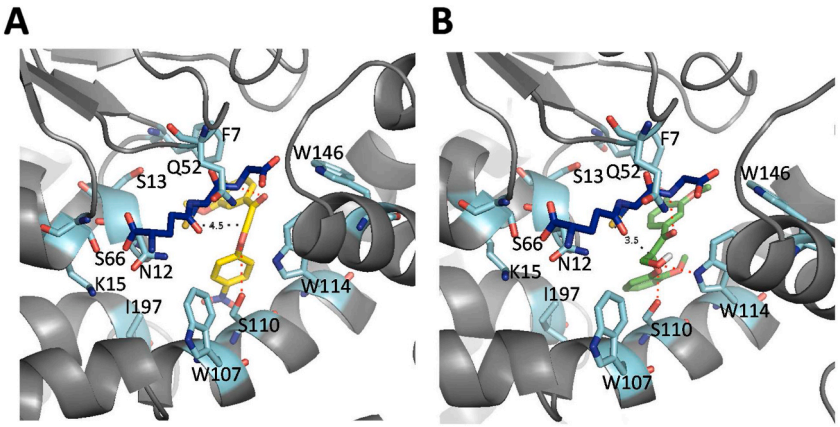

Fig. 3. Model of the ternary complex. A) LigF-AB11/GSH/PNP-AV; B) LigF-AB11/GSH/(S)-GVG. The bound glutathione (blue), docked PNP-AV (yellow), and docked (S)-GVG (green) are shown as sticks. The distance between the thiolate group in GSH and the C_β atom in the docked substrate is illustrated using a dotted line and is provided in angstroms (Å). The amino acids of the active site are displayed in cyan sticks. The red dashed lines display the hydrogen bonds between the substrate and the amino acids of the active site. (For interpretation of the references to colour in this figure legend, the reader is referred to the Web version of this article.)

(GenBank: BBC73091.1) and LigF. The selection of LigF-AB11 for further scrutiny was predicated on this high degree of similarity (Fig. 1). Furthermore, to accurately position LigF-AB11 within its evolutionary lineage, a phylogenetic tree was meticulously constructed. The foundation of this tree was rooted in an examination of other known or predicted glutathione S-transferases (GSTs) intricately associated with catalytic reactions within the sphingomonad pathway for β-aryl ether bond cleavage, as reported by Kontur et al. [17]. The findings gleaned from this analysis suggest that LigF-AB11 shares a noteworthy homology with the LigF1 subclass, aligning with the classification proposed by Kontur et al. [17] (Fig. 2).

3.2. PNP-AV as substrate of LigF-AB11 enzyme

The PNP-AV substrate was chemically synthesized as a chromogenic molecule for the enzymatic measurement of LigF-AB11 β-etherase activity. Through molecular docking analysis, it was determined that the PNP-AV molecule displayed a higher binding affinity towards the predicted protein structure of LigF-AB11 (Fig. 3A) in comparison to the (S)-GVG molecule (Fig. 3B), as evidenced by activity energy scores of −6.9 and −6.5, respectively. Notably, the orientation of PNP-AV within the enzyme's active site closely resembled that of the (S)-GVG substrate, facilitating interaction through hydrogen bonding between the substrate and the Ser110 side chain, as well as between the carbonyl oxygen Oα and the glycyl group of glutathione (Fig. 3). This suggests its potential as a valuable lignin model substrate for accurately assessing β-etherase activity. The synthesis of PNP-AV involved a nucleophilic substitution reaction between 1 g of 2-Br-1-(4-hydroxy-3-methoxyphenyl)-ethanone and a molar excess of ρ-nitrophenol (Fig. 4A). After completing the synthesis process, a product yield of 32 % was achieved, corresponding to 0.3993 g of dry weight. TLC analysis of the reaction products at 280 nm revealed the complete removal of ρ-nitrophenol, and the most intense spot corresponded to the PNP-AV substrate (Fig. 4B). The substrate was characterized using High-Performance Thin-Layer Chromatography (HPTLC) and 1D and 2D Nuclear Magnetic Resonance (NMR) spectroscopy analyses to validate its chemical identity and purity. The results revealed that PNP-AV was obtained with a purity of 37 % mol/mol, and its chemical structure was confirmed as follows: ^{1}H NMR (MeOD-d_4, 600 MHz, 298 K) 7.49 (d, $J = 2.0$ Hz, 1H, H-2), δ 6.92 (d, $J = 8.3$ Hz, 1H, H-5), 7.59 (*dd*, $J = 8.3$ and 2.0 Hz, 1H, H-6), δ 7.17 (d, $J = 8.3$ Hz, 2H, H-2′, 6′), δ 6.88 (d, $J = 8.3$ Hz, 2H, H-3′, 5′), δ 3.84 (s, 3H, OMe), δ 5.73 (s, 2H, Me); ^{13}C NMR (MeOD-d_4, 600 MHz, 298 K) δ_C 125.6 (C-1), δ_C 110.8 (C-2), δ_C 147.6 (C-3), δ_C 152.4 (C-4), δ_C 114.9 (C-5), δ_C 122.8 (C-6), δ_C 191.2 (C-7), δ_C 70.1 (C-8), δ_C 163.4 (C-1′), δ_C 115.0 (C-2′, 6′), δ_C 125.2 (C-3′, 5′), δ_C 140.8 (C-4′), δ_C 55.3 (C-3-OMe).

3.3. Expression and purification of the LigF-AB11 enzyme

The gene encoding LigF β-eterase from *Altererythrobacter* sp. B11 was inserted into the expression vector pET28a (+), resulting in a 786 bp open reading frame (ORF) (Fig. 5A). In the *E. coli* BL21 (DE3) expression system, the LigF gene yielded a mature protein consisting of 137 amino acids with a molecular weight of 31 kDa (Fig. 5B). The LigF gene (NCBI-ProteinID: BBC73091) is predicted to have a molecular mass of 28.9 kDa and an isoelectric point (*p*I) of 12.07.

The growth kinetics of *E. coli* BL21 (DE3)/LigF-AB11 exhibited an exponential phase lasting 10 h. After overnight induction at 16 °C with 0.5 mM IPTG, the cell-free culture contained approximately 2.2 g/L of the target protein (Table 1). Previous assays demonstrated the importance of maintaining a temperature of 16 °C during the induction phase to minimize *E. coli* metabolism and prevent the inclusion body formation of the expressed enzyme.

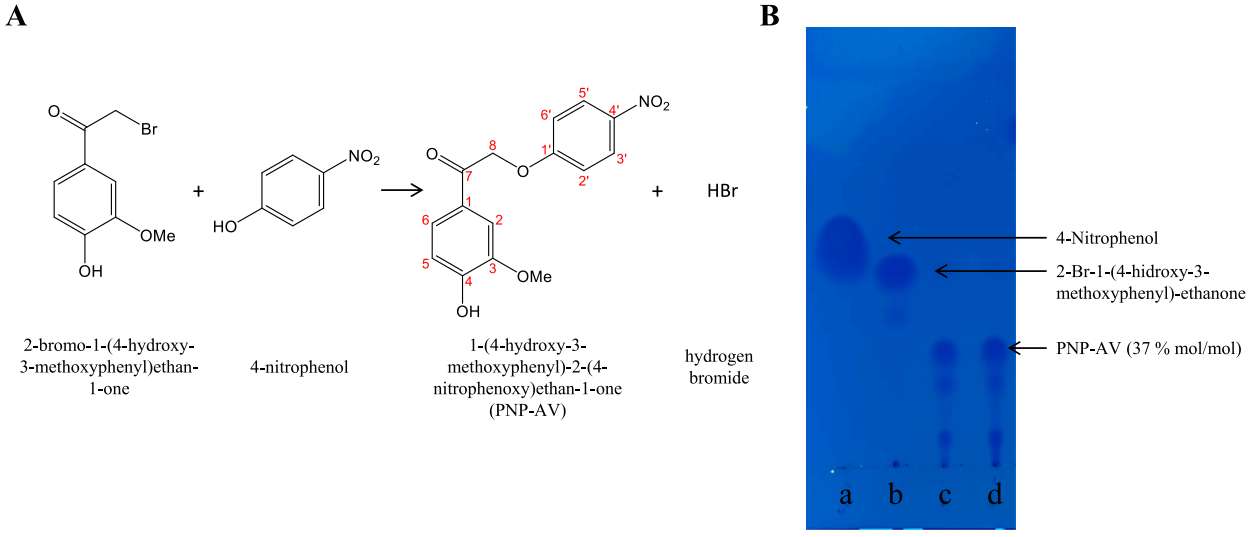

Fig. 4. Synthesis of PNP-AV substrate. A) The stoichiometric equation for PNP-AV synthesis by nucleophilic substitution reaction. B) TLC analysis of the reaction products: a) 4-Nitrophenol, b) 2-Br-1-(4-hydroxy-3-methoxyphenyl)-ethanone, c) reaction product in ethyl acetate, d) reaction product after being crystallized. Mobile phase: hexane:ethyl acetate 2:1 (v/v). Developed under UV light.

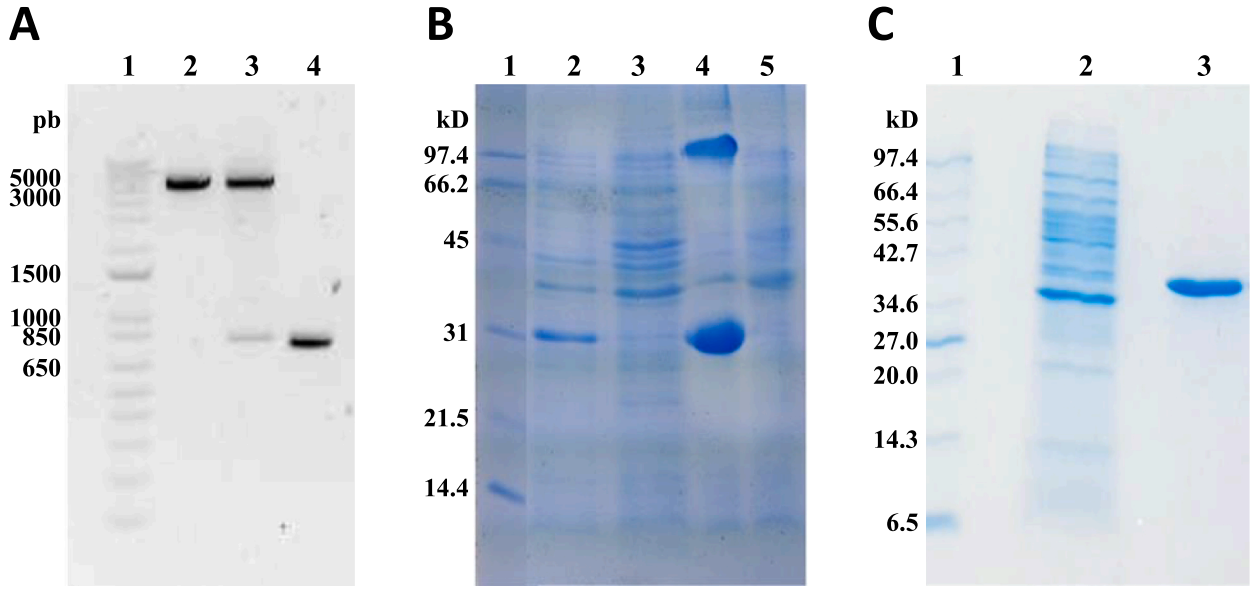

Fig. 5. Cloning, expression, and purification analysis of the β-etherase LigF-AB11 from *Altererythrobacter* sp. B11. A) Plasmid pET28/LigF-AB11 by digestion and PCR. Lanes: 1) Molecular markers, 2) Empty vector, 3) Double digest with *Nde*I and *Bam*HI, 4) PCR product of the gene. B) SDS-PAGE analysis of BL21 (DE3)/pET28 LigF-AB11 protein extract, after 12 h of induction with 1 mM IPTG at 37 °C. Lanes: 1) Molecular markers, 2) Induced soluble fraction, 3) Uninduced soluble fraction, 4) Induced insoluble fraction, 5) Uninduced insoluble fraction. C) SDS-PAGE analysis of the purification of LigF-AB11. Lanes: 1) Molecular weight markers, 2) Crude extract, 3) Pure protein.

Table 1
Purification of LigF from *Altererythrobacter* sp. B11 expressed in *E. coli* BL21 DE3)/pET-28a (+). The β-etherase activity was monitored spectrophotometrically assay at 37 °C for 15 min using PNP-AV as substrate at pH 8.0.

Purification step	Volume (mL)	Total Protein (mg)	Activity (U)	Specific activity (U/mg)	Yield (%)	Purification factor (times)
Cell-free culture	120	264 ± 12	19.019 ± 0.853	0.072 ± 0.004	100	1
His-Tag Nickel Sepharose	60	116 ± 12	11.598 ± 0.481	0.100 ± 0.003	61	1.4

The purification of the recombinant LigF-AB11 was performed using Ni-Sepharose affinity chromatography from the cell-free culture medium, specifically the crude intracellular extract (Fig. 5C). This purification method successfully allowed recovering an active enzyme with a specific activity of 0.1 U/mg and a yield of 61 %, resulting in a purification factor of 1.4 (Table 1). In a study conducted by Picart et al. [12], the purification of LigF from *Sphingobium* sp. SYK-6, expressed in *E. coli* BL21(DE3)/pET28a (+), was achieved using a nickel-nitrilotriacetic acid column. The purified enzyme exhibited a specific activity of 0.003 U/mg when measured using the fluorogenic substrate α-*O*-(*β*-methylumbelliferyl) acetovainillone [12].

3.4. Temperature and pH effects

The study on the temperature effect on the velocity of LigF-AB11 catalyzing PNP-AV substrate (Fig. 6A) revealed its mesophilic behavior, as the highest activity was observed in the assay conducted at 32 °C. Picart et al. [12] observed that recombinant enzymes LigF and LigE from *Sphingobium* sp. SYK-6, expressed in E. *coli* BL21(DE3)/pET28a (+), exhibited optimal temperatures of 25 and 30 °C, respectively. Remarkably, LigF-AB11 exhibited 87 % enzymatic activity at 18 °C compared to its maximum activity, indicating its status as a cold-active enzyme. This finding suggests a high potential for its utilization in industrial processes.

As for pH effects, LigF-AB11 reached its peak activity at pH 8.5 without displaying a plateau; in other words, the maximum activity peak was well-defined, with activity decreasing by over 30 % when the pH shifted by half a unit (Fig. 6B). Helmich et al. [13] observed that the LigF and LigE enzymes, derived from *Sphingobium* sp. SYK-6 and recombinantly expressed in the *E. coli* B834 (DE3)/pVP80K system, exhibited their optimal initial velocities at pH 8.0 and 30 °C. On the other hand, Picart et al. [12] reported that both enzymes expressed in *E. coli* BL21 (DE3)/pET28a (+) reached their optimal pH at a value of 9.0. Additionally, Wang et al. [30] observed an increased catalytic activity of LigF (expressed in *E. coli* BL21 (DE3)/pET23a) in the hydrolysis of sulfonated lignin by increasing the pH in the reaction medium, suggesting a possible relationship between enzyme-substrate binding and pH.

3.5. Stability profiles

An analysis of the stability of LigF-AB11 in the presence of PNP-AV substrate was conducted, evaluating the effect of temperature

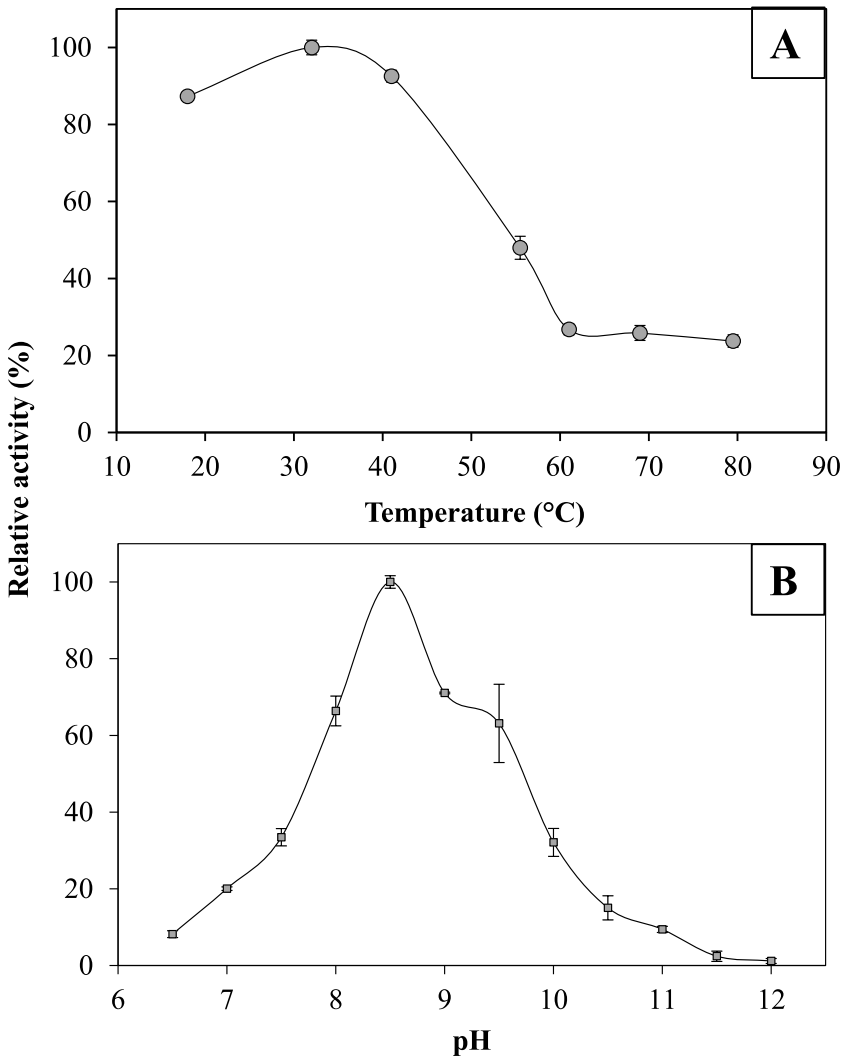

Fig. 6. Temperature and pH dependence of LigF-AB11 activity. A) Effect of temperature at pH 8.5 in 25 mM Tris-HCl buffer. B) Effect of pH at 30 °C. Assays were performed in triplicate using 0.000516 μmol of the enzyme.

and pH within different ranges. The obtained isotherms (Fig. 7A) revealed that enzymatic activity was completely lost at 60 °C in under an hour. However, LigF-AB11 maintained over 50 % residual activity at 50 °C for 1 h and retained 18 % activity after 4 h at 40 °C. These findings are reflected in the enzymatic degradation isotherms (Fig. 8), with the decay constant of activity (kd) increasing with temperature and the half-life (t½) of LigF-AB11 decreasing as temperature rises. Importantly, to the best of our knowledge, no stability studies on β-etherases had been conducted prior to this work, marking it as the pioneering investigation of its kind.

On the other hand, stability tests of LigF-AB11 at different pH levels showed that the initial activity remained stable for 1 h without significant effects when the enzyme was incubated within a pH range of 5.0–9.0. The 50 % loss of enzymatic activity occurred after 5 h (Fig. 7B). However, in highly acidic or alkaline solutions, such as pH 3.0 and 11.0, LigF-AB11 exhibited a decline of 28 % and 16 % in enzymatic activity within the first hour, respectively.

3.6. Enzyme effector assays

The effect of metal ions, including Ca^{2+}, Mn^{2+}, Na^{+}, K^{+}, Fe^{3+}, Zn^{2+}, Mg^{2+}, Hg^{2+}, and Cu^{2+}, on the activity of LigF-AB11was analyzed, and the results obtained are presented in Fig. 9A. It can be observed that certain metal ions, such as Zn^{2+}, Hg^{2+}, and Cu^{2+}, caused enzymatic inhibition in LigF-AB11, resulting in almost complete suppression of its activity. The inhibitory effects of the metal ions were observed in the following order: Zn^{2+}> Hg^{2+} >Cu^{2+} > Mn^{2+}> Fe^{3+}. Conversely, LigF-AB11 activity increased by 7–9 % when NaCl, KCl, or $MgSO_4$ were added 5 min before initiating the reaction. However, a rigorous statistical analysis using analysis of variance (ANOVA) followed by Dunnett's pairwise comparison test revealed that this increase lacks statistical significance at a 95 % confidence level.

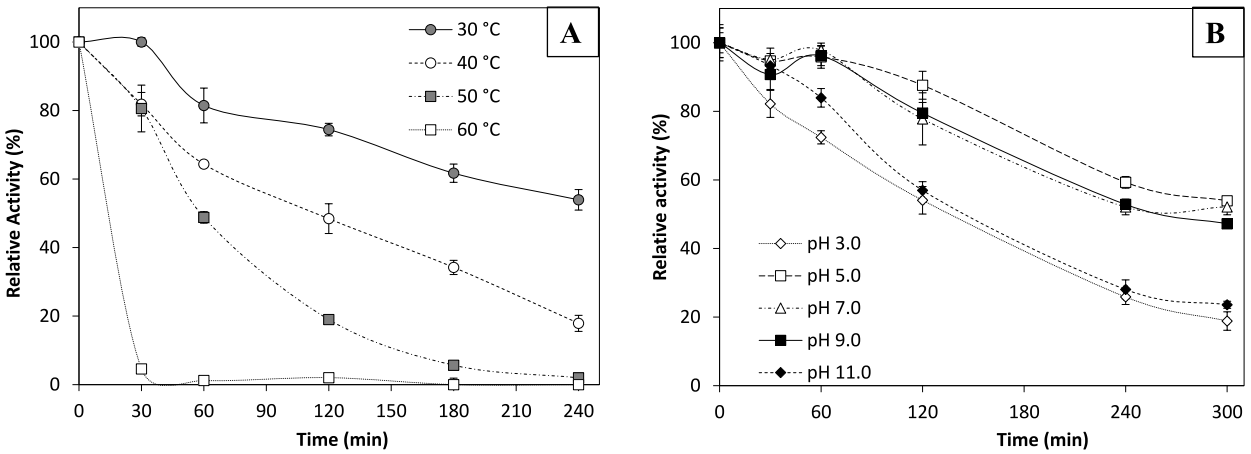

Fig. 7. Stability of LigF-AB11. A) Effect of temperature. B) Effect of pH. Assays were performed in triplicate with 0.000516 μmol of the enzyme in 50 mM Tris-HCl buffer solution at pH 8.5 and 40 mM Briton Robinson buffer solution at 25 °C, respectively. Residual activity was measured at pH 8.5.

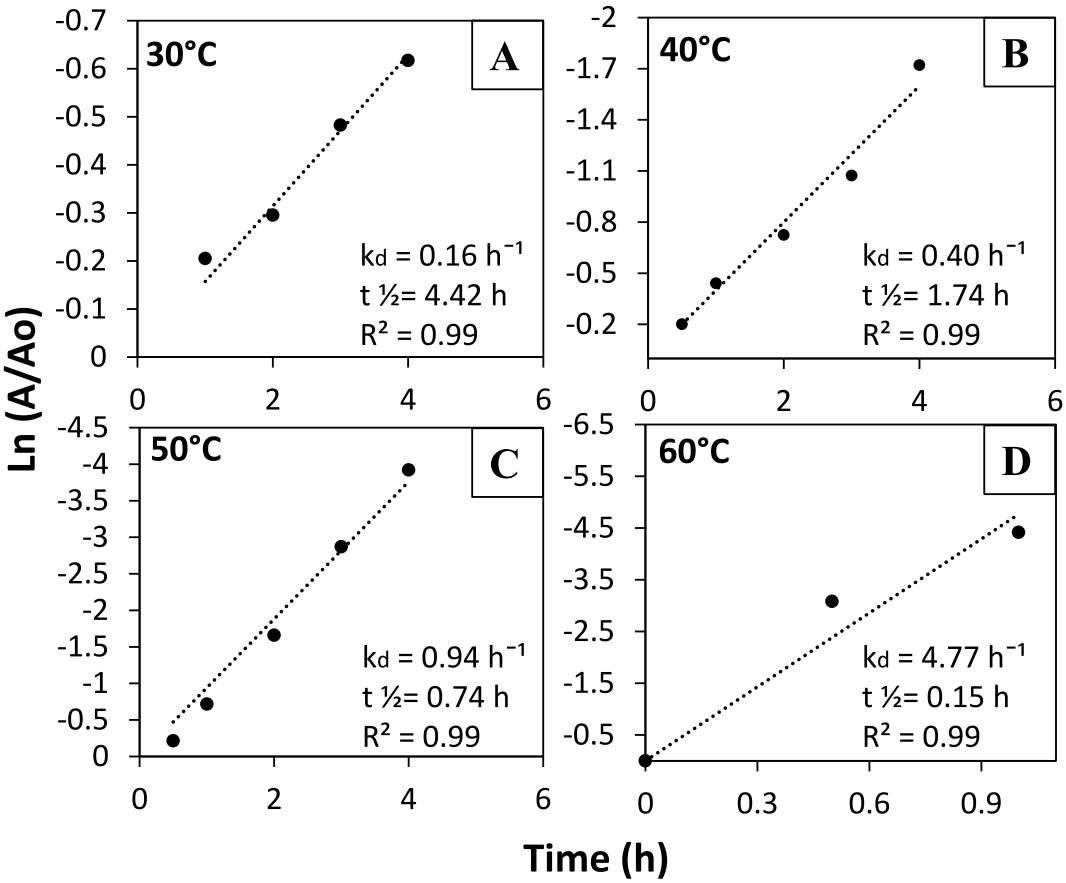

Fig. 8. Logarithm of the residual activity of LigF-A11 at different temperatures. A) 30 °C. B) 40 °C. C) 50 °C. D) 60 °C. The linear regression of the enzyme showed the first-order rate law of reaction.

The effect of metal ions on catalytic activity is of significance in the study of β-etherases since processes for lignin separation from lignocellulosic biomass may contain metals, which can impact biorefinery processes. Enzymes belonging to the Glutathione S-transferase family are known to be metal-dependent; however, their reaction rates can be inhibited or enhanced by the presence of metal ions [31]. Previous studies within this enzyme family have demonstrated inhibition of enzymatic activity in the presence of Cd^{2+},

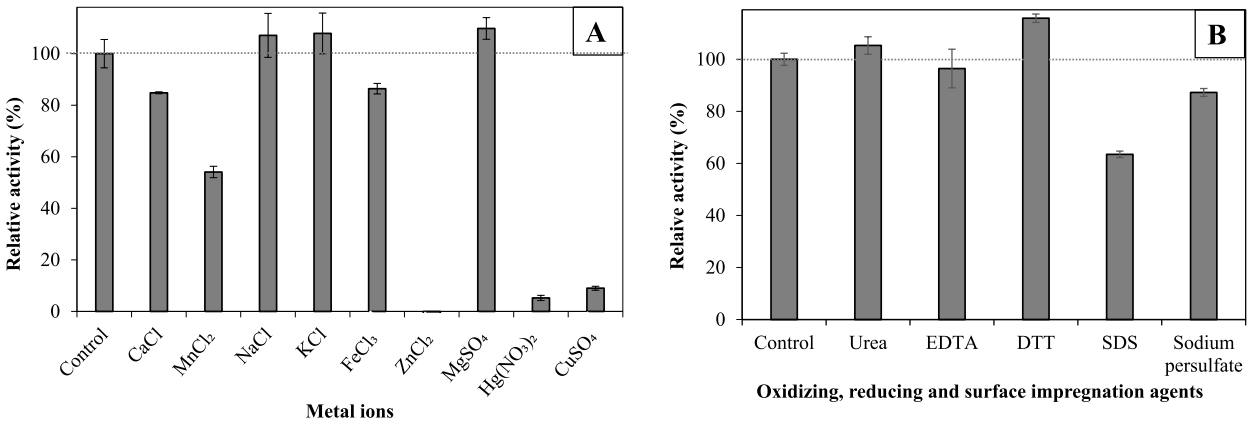

Fig. 9. Analysis of activators and inhibitors on the activity of LigF-AB11. A) Effect of metal ions (1 mM). B) Effect of oxidizing, reducing and, surface impregnation agents (0.1 mM). The enzymatic activity of LigF-AB11 was compared to a control solution without any agents.

Cu^{2+}, Zn^{2+} and, Ag^{+} [22].

Furthermore, the effects of oxidizing and reducing agents, as well as surface impregnation agents, on LigF-AB11 activity were analyzed (Fig. 9B). The protein reducing agent DTT was found to activate LigF-AB11, resulting in increased activity. Conversely, the oxidizing agent sodium persulfate had an inhibitory effect, leading to a 29 % decrease in activity. Among the surface impregnation agents tested, only SDS, a detergent known to disrupt non-covalent protein bonds, exhibited an inhibitory effect on LigF-AB11, resulting in a 37 % decrease in enzymatic activity. On the other hand, agents Urea and EDTA had no significant impact on LigF-AB11 activity, as confirmed by the Dunnett's pairwise comparison test at a 95 % confidence level.

4. Conclusions

This study offers valuable insights into the biochemical properties of the β-etherase LigF-AB11 from *Altererythrobacter* sp. B11. It has determined the optimal temperature and pH conditions, as well as the thermostability and pH stability profiles. The results underscore the pivotal role of pH in lignin biorefinery models, as evidenced by the substantial impact of the reaction medium pH on LigF-AB11 activity, with a non-plateau curve demonstrating a peak at pH 8.5. Further investigations are merited to delve into the structure-function relationship of β-etherases and unravel the underlying mechanisms governing enzyme-substrate binding. This knowledge is indispensable for advancing our comprehension in the field and optimizing the efficiency of lignin biorefinery processes.

Furthermore, the study explores the inhibitory effects of metal ions on LigF-AB11 activity. These findings hold practical significance for the development of efficient enzymatic processes for lignin depolymerization in lignin biorefineries. Subsequent studies can concentrate on refining reaction conditions and exploring the potential application of LigF-AB11 in lignin biorefinery systems. By harnessing the unique capabilities of β-etherases, it becomes feasible to enhance the conversion of lignin into value-added products, contributing to the sustainable utilization of this abundant renewable resource.

Data availability statement

Data will be made available on request.

Additional information

No additional information is available for this paper.

CRediT authorship contribution statement

Marcela Robles-Machuca: Conceptualization, Investigation, Methodology, Writing – original draft. **Lucero Aviles-Mejia:** Conceptualization, Investigation, Methodology, Writing – original draft. **Itzel Celeste Romero-Soto:** Data curation, Formal analysis, Resources, Writing – review & editing. **Jorge Alberto Rodriguez-Gonzalez:** Conceptualization, Formal analysis, Resources, Supervision, Writing – review & editing. **Vicente Paul Armenta-Perez:** Data curation, Investigation, Writing – original draft. **Maria Angeles Camacho-Ruiz:** Conceptualization, Formal analysis, Funding acquisition, Supervision, Writing – original draft, Writing – review & editing.

Declaration of competing interest

The authors declare that they have no known competing financial interests or personal relationships that could have appeared to

influence the work reported in this paper.

Acknowledgments

We appreciate the support provided by the Sectorial Research and Education Fund SEP/CONACyT, Mexico (CB-2016/283183).

References

[1] J. Becker, C. Wittmann, A field of dreams: lignin valorization into chemicals, materials, fuels, and health-care products, Biotechnol. Adv. 37 (6) (2019), 107360, https://doi.org/10.1016/j.biotechadv.2019.02.016.
[2] N. Zhou, W.P.D.W. Thilakarathna, Q.S. He, H.P.V. Rupasinghe, A review: depolymerization of lignin to generate high-value bio-products: opportunities, challenges, and prospects, Front. Energy Res. 9 (758744) (2022), https://doi.org/10.3389/fenrg.2021.758744.
[3] J. Zakzeski, P.C.A. Bruijnincx, A.L. Jongerius, B.M. Weckhuysen, The catalytic valorization of lignin for the production of renewable chemicals, Chem. Rev. 110 (6) (2010) 3552–3599, https://doi.org/10.1021/cr900354u.
[4] M.P. Pandey, C.S. Kim, Lignin depolymerization and conversion: a review of thermochemical methods, Chem. Eng. J. 34 (1) (2011) 29–41, https://doi.org/10.1002/ceat.201000270.
[5] E. Masai, Y. Katayama, S. Kubota, S. Kawai, M. Yamasaki, N. Morohoshi, A bacterial enzyme degrading the model lignin compound beta-etherase is a member of the glutathione-S-transferase superfamily, FEBS Lett. 323 (1–2) (1993) 135–140, https://doi.org/10.1016/0014-5793(93)81465-c.
[6] E. Masai, Y. Katayama, S. Kawai, S. Nishikawa, M. Yamasaki, N. Morohoshi, Cloning and sequencing of the gene for a Pseudomonas paucimobilis enzyme that cleaves beta-aryl ether, J. Bacteriol. 173 (24) (1991) 7950–7955, https://doi.org/10.1128/jb.173.24.7950-7955.1991.
[7] P. Picart, P. Domínguez de María, A. Schallmey, From gene to biorefinery: microbial β-etherases as promising biocatalysts for lignin valorization, Front. Microbiol. 6 (916) (2015), https://doi.org/10.3389/fmicb.2015.00916.
[8] E. Adler, Lignin chemistry—past, present and future, J. Indian Acad. Wood Sci. 11 (3) (1977) 169–218, https://doi.org/10.1007/BF00365615.
[9] Y. Sato, H. Moriuchi, S. Hishiyama, Y. Otsuka, K. Oshima, D. Kasai, M. Nakamura, S. Ohara, Y. Katayama, M. Fukuda, E. Masai, Identification of three alcohol dehydrogenase genes involved in the stereospecific catabolism of arylglycerol-beta-aryl ether by Sphingobium sp. strain SYK-6, Appl. Environ. Microbiol. 75 (16) (2009), https://doi.org/10.1128/aem.00880-09.
[10] E. Masai, A. Ichimura, Y. Sato, K. Miyauchi, Y. Katayama, M. Fukuda, Roles of the enantioselective glutathione S-transferases in cleavage of beta-aryl ether, J. Bacteriol. 185 (6) (2003) 1768–1775, https://doi.org/10.1128/jb.185.6.1768-1775.2003.
[11] D.L. Gall, J. Ralph, T.J. Donohue, D.R. Noguera, A group of sequence-related sphingomonad enzymes catalyzes cleavage of β-aryl ether linkages in lignin β-guaiacyl and β-syringyl ether dimers, Environ. Sci. Technol. 48 (20) (2014) 12454–12463, https://doi.org/10.1021/es503886d.
[12] P. Picart, C. Müller, J. Mottweiler, L. Wiermans, C. Bolm, P. Domínguez de María, A. Schallmey, From gene towards selective biomass valorization: bacterial β-etherases with catalytic activity on lignin-like polymers, ChemSusChem 7 (11) (2014) 3164–3171, https://doi.org/10.1002/cssc.201402465.
[13] K.E. Helmich, J.H. Pereira, D.L. Gall, R.A. Heins, R.P. McAndrew, C. Bingman, K. Deng, K.C. Holland, D.R. Noguera, B.A. Simmons, K.L. Sale, J. Ralph, T. J. Donohue, P.D. Adams, G.N. Phillips Jr., Structural basis of stereospecificity in the bacterial enzymatic cleavage of β-aryl ether bonds in lignin, J. Biol. Chem. 291 (10) (2016) 5234–5246, https://doi.org/10.1074/jbc.M115.694307.
[14] T. Fukuzumi, H. Takatuka, K. Minami, Enzymic degradation of lignin V. The effect of NADH on the enzymic cleavage of arylalkylether bond in veratrylglycerol-β-guaiacylether as lignin model compound, Arch. Biochem. Biophys. 129 (1) (1969) 396–403, https://doi.org/10.1016/0003-9861(69)90191-X.
[15] R.L. Crawford, T.K. Kirk, J.M. Harkin, E. McCoy, Bacterial cleavage of an arylglycerol- -aryl ether bond, Appl. Environ. Microbiol. 25 (2) (1973) 322–324, https://doi.org/10.1128/am.25.2.322-324.1973.
[16] E. Masai, Y. Katayama, S. Nishikawa, M. Yamasaki, N. Morohoshi, T. Haraguchi, Detection and localization of a new enzyme catalyzing the beta-aryl ether cleavage in the soil bacterium (Pseudomonas paucimobilis SYK-6), FEBS Lett. 249 (2) (1989) 348–352, https://doi.org/10.1016/0014-5793(89)80656-8.
[17] W.S. Kontur, C.N. Olmsted, L.M. Yusko, A.V. Niles, K.A. Walters, E.T. Beebe, K.A. Vander Meulen, S.D. Karlen, D.L. Gall, D.R. Noguera, T.J. Donohue, A heterodimeric glutathione S-transferase that stereospecifically breaks lignin's β(R)-aryl ether bond reveals the diversity of bacterial β-etherases, J. Biol. Chem. 294 (6) (2019) 1877–1890, https://doi.org/10.1074/jbc.RA118.006548.
[18] J. Reiter, H. Strittmatter, L.O. Wiemann, D. Schieder, V. Sieber, Enzymatic cleavage of lignin β-O-4 aryl ether bonds via net internal hydrogen transfer, Green Chem. 15 (5) (2013) 1373–1381, https://doi.org/10.1039/C3GC40295A.
[19] H. Voß, C.A. Heck, M. Schallmey, A. Schallmey, Database mining for novel bacterial β-etherases, glutathione-dependent lignin-degrading enzymes, Appl. Environ. Microbiol. 86 (2) (2020), https://doi.org/10.1128/aem.02026-19.
[20] P. Picart, H. Liu, P.M. Grande, N. Anders, L. Zhu, J. Klankermayer, W. Leitner, P. Domínguez de María, U. Schwaneberg, A. Schallmey, Multi-step biocatalytic depolymerization of lignin, Appl. Microbiol. Biotechnol. 101 (15) (2017) 6277–6287, https://doi.org/10.1007/s00253-017-8360-z.
[21] M.M. Cajnko, J. Oblak, M. Grilc, B. Likozar, Enzymatic bioconversion process of lignin: mechanisms, reactions and kinetics, Bioresour. Technol. 340 (2021), https://doi.org/10.1016/j.biortech.2021.125655.
[22] M.S. Özaslan, Y. Demir, O.I. Küfrevioğlu, M. Çiftci, Some metals inhibit the glutathione S-transferase from Van Lake fish gills, J. Biochem. Mol. Toxicol. 31 (11) (2017), https://doi.org/10.1002/jbt.21967.
[23] D.S. Auld, [11] Use of chelating agents to inhibit enzymes, in: Methods in Enzymology, Academic Press, 1988, pp. 110–114, https://doi.org/10.1016/0076-6879(88)58051-5.
[24] J.C. Pereira, E.C. Giese, M.M.S. Moretti, A.C.S. Gomes, O.M. Perrone, M. Boscolo, R. Da Silva, E. Gomes, D.A.B. Martins, Effect of metal ions, chemical agents and organic compounds on lignocellulolytic enzymes activities, in: S. Murat (Ed.), Enzyme Inhibitors and Activators, IntechOpen: Rijeka, 2017, https://doi.org/10.5772/65934. Ch. 6.
[25] A.H. Maeda, S. Nishi, S. Ishii, Y. Shimane, H. Kobayashi, J. Ichikawa, K. Kurosawa, W. Arai, H. Takami, Y. Ohta, Complete genome sequence of altererythrobacter sp. strain B11, an aromatic monomer-degrading bacterium, isolated from deep-sea sediment under the seabed off kashima, Japan, Genome Announc. 6 (12) (2018), https://doi.org/10.1128/genomeA.00200-18.
[26] D.J. Levy-Booth, A. Hashimi, R. Roccor, L.-Y. Liu, S. Renneckar, L.D. Eltis, W.W. Mohn, Genomics and metatranscriptomics of biogeochemical cycling and degradation of lignin-derived aromatic compounds in thermal swamp sediment, ISME J. 15 (3) (2021) 879–893, https://doi.org/10.1038/s41396-020-00820-x.
[27] M.D. Hanwell, D.E. Curtis, D.C. Lonie, T. Vandermeersch, E. Zurek, G.R. Hutchison, Avogadro: an advanced semantic chemical editor, visualization, and analysis platform, J. Cheminf. 4 (1) (2012) 17, https://doi.org/10.1186/1758-2946-4-17.
[28] O. Trott, A.J. Olson, AutoDock Vina, Improving the speed and accuracy of docking with a new scoring function, efficient optimization, and multithreading, J. Comput. Chem. 31 (2) (2010) 455–461, https://doi.org/10.1002/jcc.21334.
[29] G.M. Morris, R. Huey, W. Lindstrom, M.F. Sanner, R.K. Belew, D.S. Goodsell, A.J. Olson, AutoDock4 and AutoDockTools4: automated docking with selective receptor flexibility, J. Comput. Chem. 30 (16) (2009) 2785–2791, https://doi.org/10.1002/jcc.21256.
[30] C. Wang, X. Ouyang, S. Su, X. Liang, C. Zhang, W. Wang, Q. Yuan, Q. Li, Effect of sulfonated lignin on enzymatic activity of the ligninolytic enzymes Cα-dehydrogenase LigD and β-etherase LigF, Enzym. Microb. Technol. 93–94 (2016) 59–69, https://doi.org/10.1016/j.enzmictec.2016.07.008.
[31] E.V.P. Medyantseva, M.G. Vertlib, G.K. Budnikov, Metal ions as enzyme effectors, Ruso. Química. Rev. 67 (3) (1998) 225–232, https://doi.org/10.1070/RC1998v067n03ABEH000228.